THE EFFECT OF VACANCY CONCENTRATION ON HYDROGEN DIFFUSION IN ALPHA-FE BY MOLECULAR DYNAMICS

Xiongying Li, Yongzhi Zhao, Jinyang Zheng*, Chaohua Gu, Ruihuan Cai

Institute of Process Equipment, Zhejiang University, Hangzhou 310027, Zhejiang, P. R. China, jyzh@zju.edu.cn

ABSTRACT

Diffusion coefficient is in significant dependence on vacancy concentration due to that migration of vacancy is the dominant mechanism of atom transport or diffusion in processes, such as void formation, dislocation movement and solid phase transformation. This study aims to investigate the effect of vacancy concentration on hydrogen diffusion in alpha-Fe by molecular dynamics simulations, especially at low temperatures and with loading. Comparisons of the diffusion coefficients between alpha-Fe with a perfect structure and different-concentration vacancies, as well as comparisons between experimental and theoretical results had been made to characterize and summarize the effect of vacancy on hydrogen diffusion coefficient.

1.0 INTRODUCTION

Hydrogen has attracted extensive attention from governments and enterprises [1,2]. On the one hand, the increasing energy crisis and environmental pollution issues have promoted the rapid development of clean energy, such as hydrogen. On the other hand, hydrogen has been regarded as an effective clean energy and displayed promising applications due to its advantages, such as abundance in sources, convenience for storage and transport, high combustion value and zero discharge. However, hydrogen embrittlement (HE) is an inevitable issue and plays a key role in the exposure accidence of applications in high pressure hydrogen storage system. Therefore, with the perspective of either physical mechanism or engineering applications, it is quite necessary to reveal the HE of materials that typically used in high pressure hydrogen storage system, especially Fe-based alloys.

Hydrogen diffusion in iron has been considerably discussed [3-10], because of that hydrogen diffusion is the essential of mass transfer process in determining the microstructure evolutions and mechanical behaviors of materials, and the precondition for the occurrence of HE. Controversy however has existed in the hydrogen diffusion in iron at low temperatures (below 500 K). For example, the hydrogen diffusion at room temperature ranges from 10^{-8} to 10^{-5} cm^2/s [5,11]. The large scatter of the results is possibly caused by surface effects and trapping effects. At high temperatures, the interference from surface inhibition reactions, surface effects and trapping effects are avoidable by a time-lag technique, which is an effective method to measure the accurate hydrogen diffusion coefficient [8]. At low temperatures, the electrochemical hydrogen permeation technique [8,12] is a suitable method for the determination of hydrogen diffusivity due to its ability to avoid surface effects. However, trapping effects resulted from lattice imperfections, such as impurities, dislocations, vacancies and microvoids, are inevitable and all significantly related to the scattered results, leading to the difficulty in accurate measurements of hydrogen diffusion. Evaluating the effect of every trap is another difficulty in accurately determining the hydrogen diffusion coefficient. Nevertheless, an effectively experimental method towards this difficulty is still missing.

Vacancy is one typically-existing trap for hydrogen and plays an important role in the HE of metals. Nagano et al. have reported that vacancy-hydrogen bubbles may be particularly important in hydrogen based on their thermal desorption investigations, which strongly suggest that the susceptibility of a materials to HE is in dependence of vacancy clusters [13,14]. This vacancy-assisted mechanism may be the dominant reason of HE in iron under normal operating conditions [15] where the previous proposed HE mechanisms [16-18] do not provide a reasonable explanation. Moreover, it is evident from numerous measurements that hydrogen penetration into iron results in the superabundance of

vacancies [19-21], leading to the formation of vacancy clusters or microvoids. These clusters and microvoids are internally stabilized by hydrogen atoms [22], and such stabilization effect results in the enhanced plasticity or ductile fracture. Hence, a thorough understanding of the vacancy-hydrogen interaction is essential to the determination of the role that vacancy plays in HE.

The above-mentioned findings inspire us to investigate the effect of vacancy concentration on the hydrogen diffusion in α-Fe by molecular dynamics (MD) simulation method which is effective to describe the vacancy-hydrogen interaction due to the exclusion of the effects from other types of traps, such as dislocation, impurities, grain boundaries and phase boundaries. As a step towards this goal, the present work had carried out MD simulations on the diffusion behavior of H into α-Fe with a perfect body-centered cubic (BCC) structure and three types of defective structures resulted from the existence of different vacancy concentrations. Both qualitative and quantitative analysis have been conducted on the influence of vacancy on hydrogen diffusion behavior with and without tension at a large scale of temperatures.

2.0 METHODS

Table 1. The concentration of vacancies (C^{V}) in alpha-Fe.

N^{V}	0	48	87	131
N^{Fe}	2590	2542	2503	2459
C^{V} (at. %)	0	1.89	3.48	5.33

Figure 1 shows the schematic of simulation models and boxes. In all systems, 518 hydrogen atoms adsorb on the top and bottom (110) surfaces of α-Fe. The number of other atoms and vacancy concentration are given in Table 1. Single vacancies uniformly distribute within the α-Fe. Periodic boundary is applied on the *x* and *y* directions. The two ends of Fe with every in the length of about 6 Å along the *x* axis is fixed. The tension loading with a speed of 5.169×10^{-3} Å/ps (that is 10^{8}/s in the strain speed) is applied on the fixed Fe atoms. A deformation of 20% is applied for all the cases that Fe is subjected to tension loading.

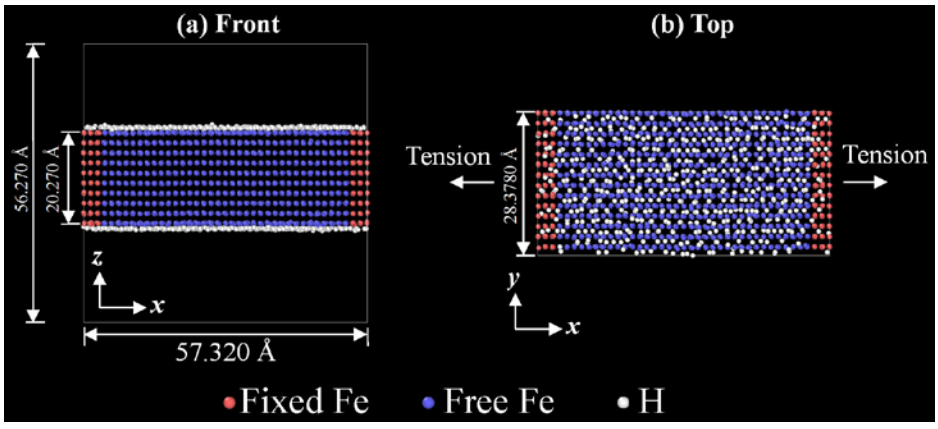

Figure 1. Schematic of the initial simulation models: (a) the front view and (b) the top view.

Atomistic interactions are calculated the modified embedded-atom method (MEAM) potential [23] due to its accuracy in reproducing the known physical properties (i.e. vacancies, dislocations, and grain boundaries) for H-Fe system. MD simulations are carried out in the constant-volume and constant-temperature (NVT) ensemble with the temperature ranging from 100 K to 900 K controlled

by the Nose-Hoover method [24]. It is noted that the initial simulation models are created at 300 K, then the temperature increases or decreases at a speed of 1.0 K/ps to the desired temperatures. Every MD simulation at the constant temperature is run for 1000 ps. The time integration of Newton's equation of motion is undertaken using the velocity Verlet algorithm [25] to evolve the system at a time step of 0.5 fs. All the trajectories are propagated by using the large-scale Atomic/Molecular Massively Parallel Simulator (LAMMPS) package [26]. The diffusion coefficient (D) of hydrogen atom is derived from the mean square displacement (MSD)-time curve according to the Einstein diffusion law: $D = \lim_{t\to\infty} \frac{\left\langle \left| r_i(t) - r_i(0) \right|^2 \right\rangle}{6t}$, where $ri(t)$ is the position of the atom i at the time t, $\langle \cdots \rangle$ denotes an average over all hydrogen atoms.

3.0 RESULTS AND DISCUSSION

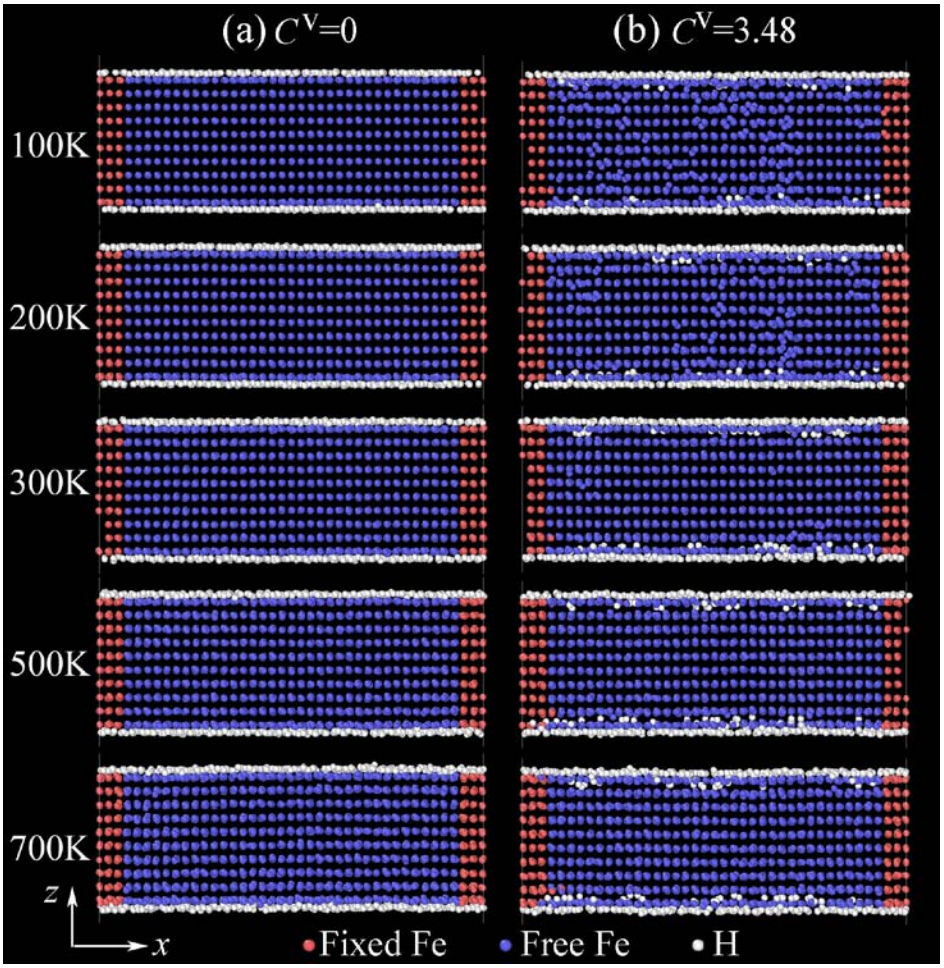

Figure 2. Equilibrium snapshots of final states (after a 1000 ps MD run) of the Fe-H system with (a) C^V=0 at. %and (b) C^V=3.48 at. % at temperatures from 100 to 700 K.

Figure 2 shows the equilibrium snapshots of final states (after a 1000 ps MD run) of the Fe-H system with C^V=0 and 3.48 at. % at different temperatures, as a representative for the comparison of hydrogen diffusion behavior between the cases with and without vacancies. As for the cases C^V=0, no penetrating hydrogen atoms into Fe with a perfect BCC structure are observed, meaning that it is quite difficult for hydrogen atoms diffuse into perfect-structure BCC Fe. Due to the low potential

energy and stability of the perfect structure, Fe does not deform when interacts with hydrogen atoms. The deformation energy is the driving energy for the penetration of hydrogen atoms into metals. In terms of the case with vacancies, Fe deforms, leading to the fluctuation of the energy of the Fe lattice. The lattice distortion energy provides the energy for the diffusion of hydrogen atoms into Fe lattice. For the example C^{V} =3.48 at. %, partial adsorbed hydrogen atoms diffuse into the Fe lattice. Moreover, the quantitative of diffusing atoms increases with the increasing temperature, as shown in Figure 2b.

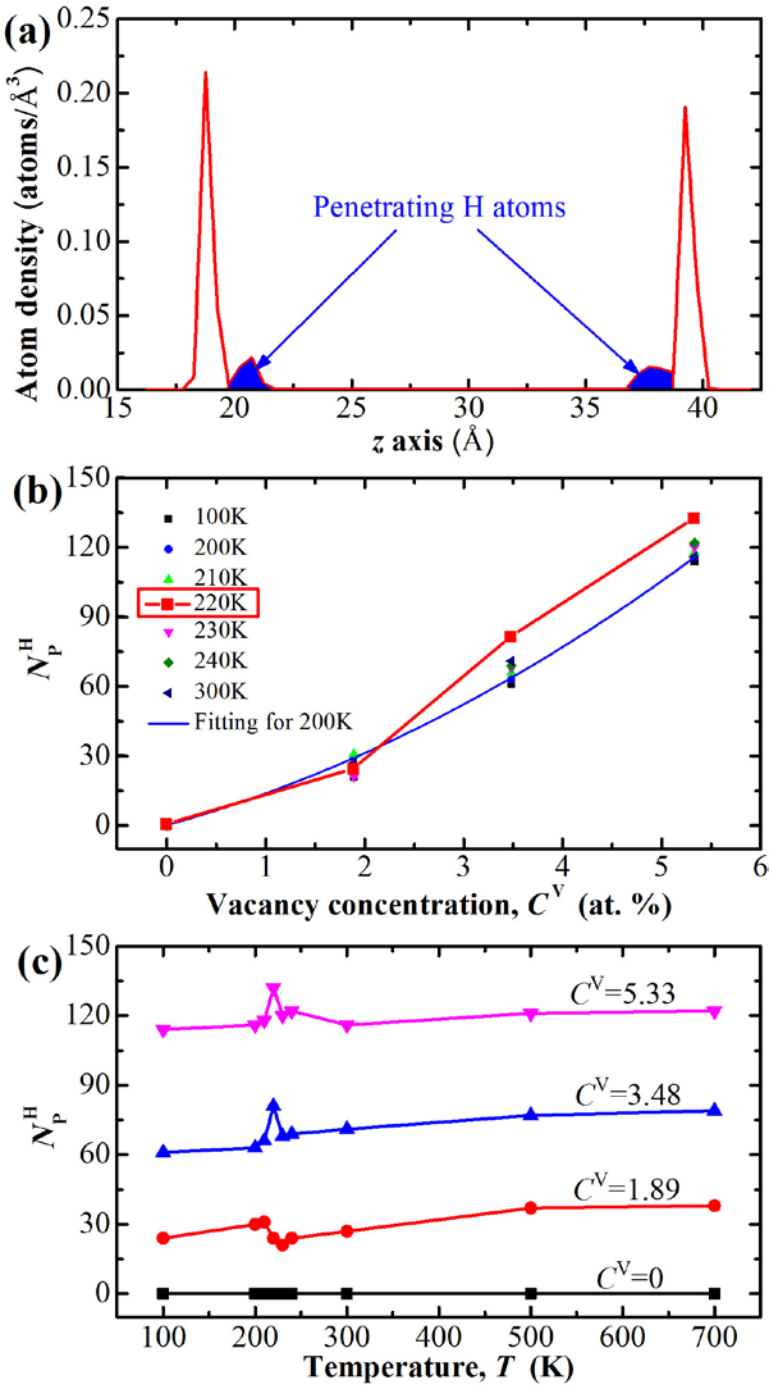

Figure 3. The relations of the number of diffusing hydrogen atoms (N_P^H) versus vacancy concentration (C^V) and temperature (T).

In order to quantitatively analyze the influences of vacancy concentration and temperature on the diffusion of hydrogen, the atom density distribution of hydrogen along the *z* direction is given in Figure 3a. Obvious four peaks are observed in the atom density curve. The first left and first right peaks present the adsorbed hydrogen on the top and bottom surfaces of Fe, and the other two peaks present the disusing hydrogen. The number of diffusing hydrogen atoms, $N_{\mathrm{P}}^{\mathrm{H}}$, are measured by integrating the two low peaks, as indicated by the blue parts in Figure 3a. Figure 3b shows the relation between the $N_{\mathrm{P}}^{\mathrm{H}}$ and vacancy concentration. Clearly, the $N_{\mathrm{P}}^{\mathrm{H}}$ displays an increasing tendency with the increasing vacancy concentration, and the relation can be fit by a quadratic function except for the case T=220 K, as indicated by the blue line, which is given as an example. This can be explained by that the release of the lattice distortion energy increases with the increasing temperature, as indicated by Figure 2b, in which remarkable lattice distortion areas are observed when the system reaches the equilibrium after a long MD run. As for the case T=220 K, the relation between the $N_{\mathrm{P}}^{\mathrm{H}}$ and vacancy concentration does not abide by a quadratic function due to the significant increase of the $N_{\mathrm{P}}^{\mathrm{H}}$ when the C^{V} is larger than 3.48 at. %. For the further analysis of the influence of temperature on the $N_{\mathrm{P}}^{\mathrm{H}}$, the relation between the $N_{\mathrm{P}}^{\mathrm{H}}$ and temperature is given in Figure 3c. The larger the C^{V} is, the higher the $N_{\mathrm{P}}^{\mathrm{H}}$ is. Moreover, the $N_{\mathrm{P}}^{\mathrm{H}}$ slightly increases with the increasing temperature except for the ceases near the temperature T=220 K. Near the temperature T=220 K, the $N_{\mathrm{P}}^{\mathrm{H}}$ decreases when C^{V}=1.89 at. % and significantly increases when the C^{V} is larger than 3.48 at. %, suggesting that the $N_{\mathrm{P}}^{\mathrm{H}}$ is quite sensitive to vacancy concentration, especially for the cases near the temperature T=220 K and the cases that C^{V} is larger than 3.48 at. %. Hence, it can be concluded from Figure 3 that: 1) the $N_{\mathrm{P}}^{\mathrm{H}}$ is sensitive to vacancy concentration and temperature, especially near the temperature T=220 K and when the C^{V} is larger than 3.48 at. %.

Table 2. Fracture of the Fe-H system subjected to tension loading.

⋈: Fracture ⋈: Brittle fracture ◆: Abnormal fracture				
T(K)	C^{V}(at. %)			
	0	1.89	3.48	5.33
100		◆	⋈	⋈
200	⋈		⋈	⋈
210	⋈	◆		⋈
220	⋈	⋈	⋈	⋈
230	⋈	◆	⋈	⋈
240		◆	⋈	⋈
300		◆	⋈	⋈
500				
700	◆			

Tensile properties of the Fe-H systems with and without vacancies at different temperatures had been studied, and the corresponding results are shown in Table 2. All of the systems are subjected to a 20% tensile deformation at a speed of 5.169×10^{-3} Å/ps (that is 10^{8}/s in the strain speed). Four types of results for the Fe-H systems are observed: 1) plastic fractures occurring near the center areas (marked by the blue symbols), 2) brittle fractures (marked by red symbols), 3) plastic fractures occurring at the areas near two fixing ends (named abnormal fractures and marked by black symbols) and 4) no fractures occurring (marked by blanks). It can be found that fractures are observed at low temperatures (below 300 K) rather than at high temperatures (above 300 K) and quite sensitive to vacancy concentration and temperature. It is worthy of noting that brittle fractures easily occur when C^{V}=3.48

or at the scale T=100~240 K, especially T=210~220 K. Therefore, it can be concluded from the statistical results in Table 2 that both the temperature scale T=210~220 K and the vacancy concentration C^{V}=3.48 are high frequency areas for brittle fractures.

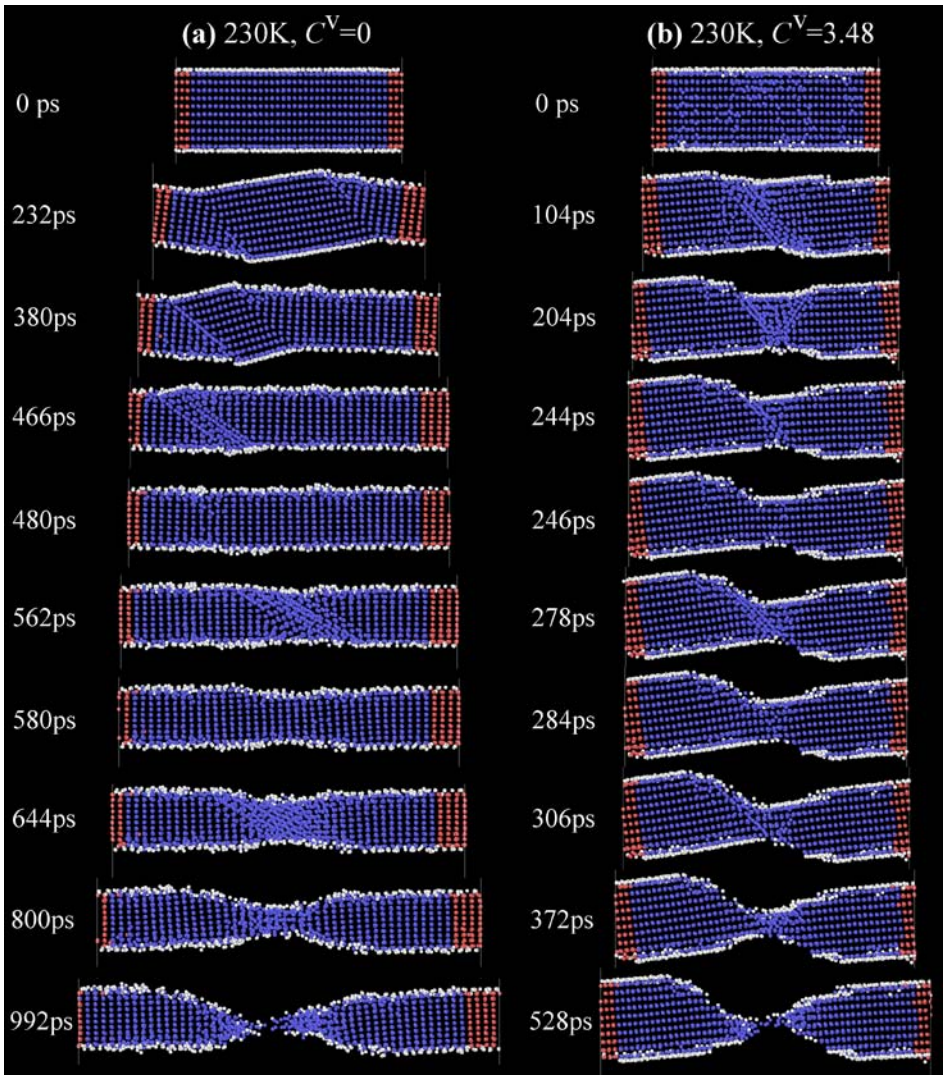

Figure 4. Equilibrium snapshots of final states (after a 1000 ps MD run) of the Fe-H system with (a) C^{V}=0 at. %and (b) C^{V}=3.48 at. % at temperatures from 100 to 700 K.

The characteristics of plastic and brittle fractures in this work are shown in Figure 4. Here, the snapshots of the cases C^{V}=0 and 3.48 at 230 K are exhibited as examples for the plastic and brittle fractures. As for the case C^{V}=0, the fracture process occurs at the following steps: 1) a glide plane generates at every end, 2) the two glide planes move to each other and meet (at 466 ps), then disappear (at 480 ps), resulting in the change of the lattice structure, 3) the second slippage occurs at the centre area or at the area near the two ends (at 562 ps), then disappears again (at 580 ps), 4) the final slippage occurs near the centre area until the Fe-H system fractures. Hence, the characteristics of plastic fracture are that: a) the occurrence of the change in the lattice structure after the first slippage, b) the slippages generate at different areas. While for the case C^{V}=3.48, a) the first slippage generates without the change of the lattice structure, b) all the slippages generate at a same place, resulting in a rapid fracture, c) the fracture surface seems to be a plane quite different from the hook face of the plastic fracture, d) the plastic deformation area (near the fracture surface) is far smaller than that of the

brittle fracture. Hence, in this work, all the fractures with similar characteristics to that of the case C^{V}=0 are defined as plastic fractures, and the fractures with similar characteristics to that of the case C^{V}=3.48 are defined as brittle fractures.

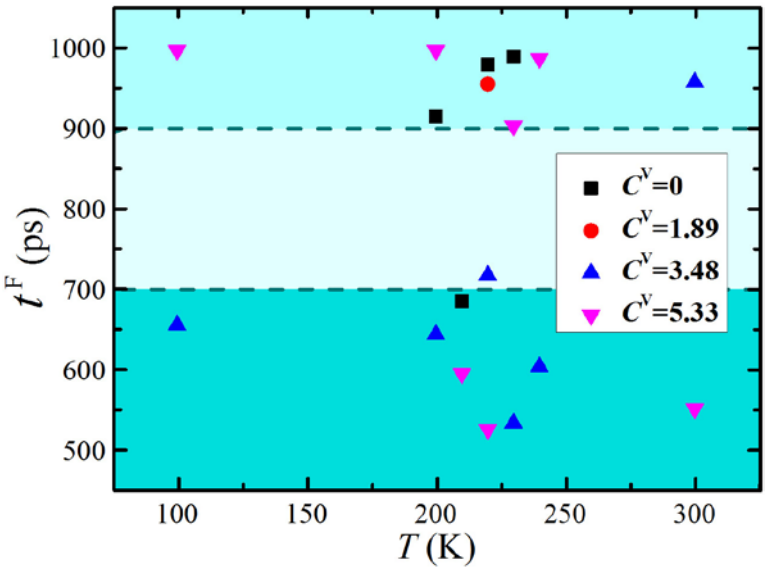

Figure 5. Fracture time (t^{F}) versus temperature for the Fe-H systems subjected to the tensile loading at a speed of 5.169×10^{-3} Å/ps.

The fracture time are measured to quantitatively analyze the effects of vacancy concentration and temperature on the tensile properties of the Fe-H systems, as shown in Figure 5. As for the plastic fractures, fractures nearly occur at the time before 700 ps, about 22.2% earlier than that of brittle fractures, which occur above 900 ps, replying the high sensitivity of brittle fracture to vacancy concentration, especially when C^{V}=3.48.

Diffusion coefficient is an important parameter to investigate the diffusion behavior of hydrogen atoms. Here, the diffusion coefficient of hydrogen atoms, D^{H}, is obtained by deriving from the MSD-*t* curve based on the function given in the method section. When the simulation system reaches too the equilibrium, the MSD shows a linear relation with time, *t*, and the slop of the linear curve is the diffusion coefficient. Figure 6a gives the MSD-*t* curves of partial cases for examples. The corresponding diffusion coefficients deriving from Figure 6a are shown in Figure 6b. According to Fick's law of diffusion, the ln*D* is linear to 1/*T*. However, in this work, Figure 6b shows that the D^{H} displays a linear relation with temperature but with different slops at low and high temperatures. At low temperatures (T≦300 K), our simulation results are quite similar to that from Ref. 5. While at high temperatures (T>300 K), the D^{H} increases more rapidly than that from other experimental results. This possibly because of the integration of vacancies, leading the enhancement of the diffusion of hydrogen atoms.

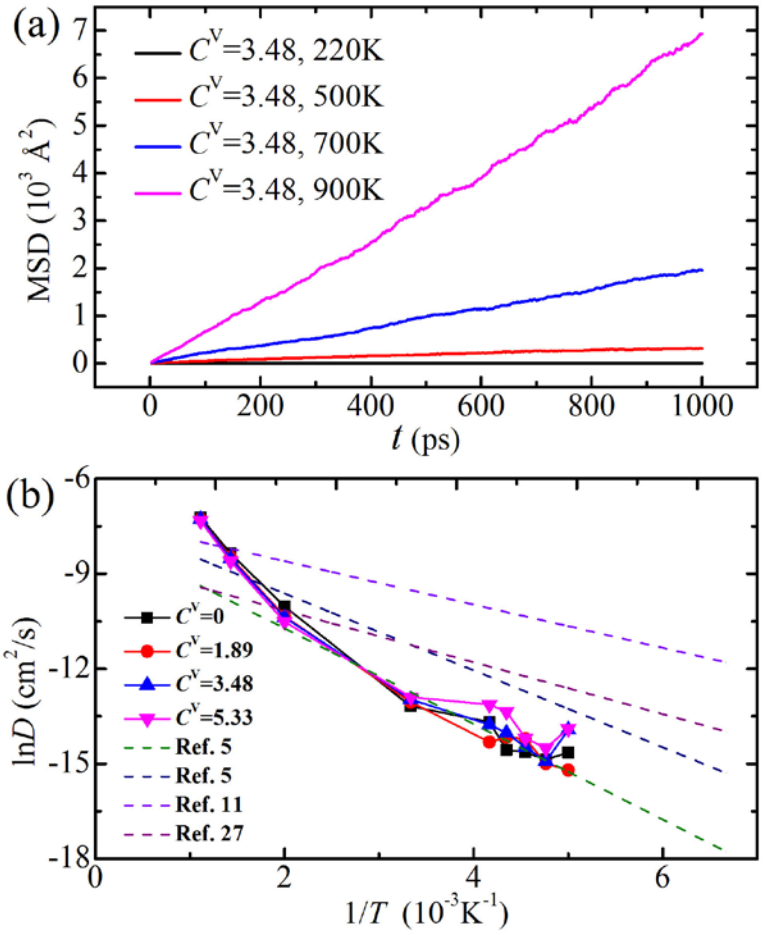

Figure 6. Diffusion coefficient of hydrogen atoms for the Fe-H systems without tensile loading at temperatures from 200 to 900 K.

Figure 7 shows the diffusion coefficient of hydrogen atoms for the Fe-H systems subjected to tensile loading. Figure 7a shows that the MSD increases with time, but does not displays a linear relation with time, because the Fe-H systems are in a nonequilibrium state during the tension process. Here, the instantaneous diffusion coefficient at the time scale from 400 to 600 ps (marked by oblique line zone in Figure 7a) before fracture is measured to characterize the diffusion behavior at the condition with tensile loading, as shown in Figure 7b. Results show that the D^H is far larger than that obtained at the condition without tensile loading, indicating the significant enhancement of diffusion behavior of hydrogen atoms at the condition with loading. The results here are also much higher than the experimental results [5,11,27], possibly due to the much higher tension speed here than that used in experiments. Besides, the ln$D$ is nearly linear to 1/T except for the fluctuation near the temperature T=220 K. At the temperature scale 210-230 K, the D^H slightly increases for the cases C^V=3.48 and 5.33 at. %, but slightly decreases for the case C^V=1.89 at. %, which provides a proof for the high sensitivity of brittle fracture at this time scale and at high vacancy concentration, especially C^V=3.48. Therefore, it can be concluded from Figure 7 that both the temperature scale T=210~230 K and the vacancy concentration C^V=3.48 are high frequency areas for brittle fractures from the perspective of diffusion coefficient.

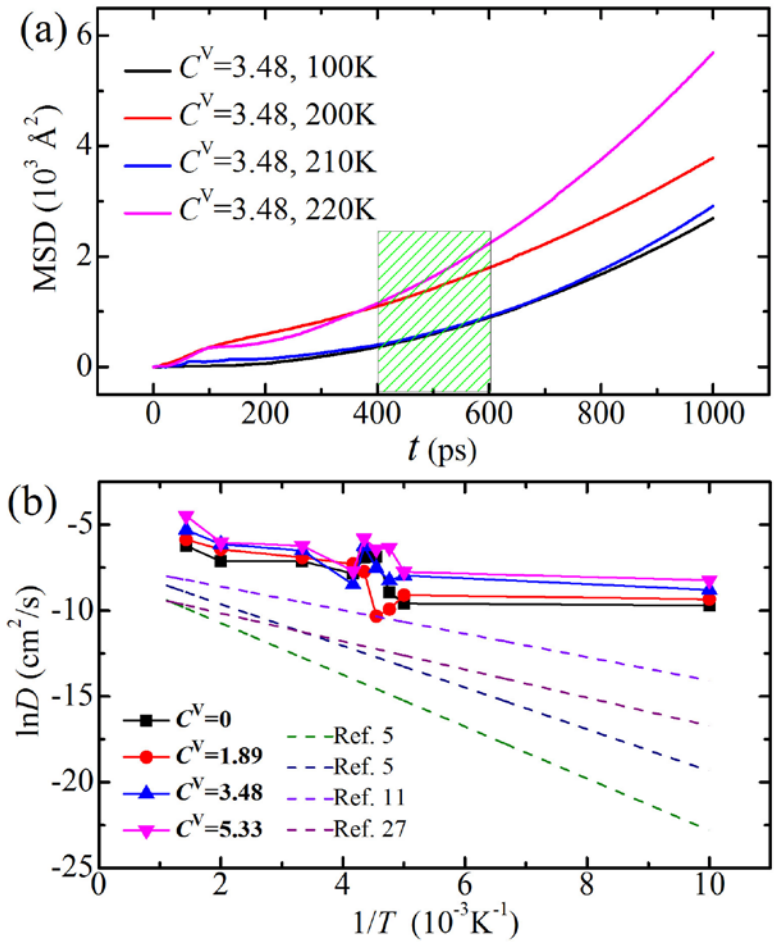

Figure 7. Diffusion coefficient of hydrogen atoms for the Fe-H systems subjected to tensile loading at temperatures from 100 to 700 K.

4.0 CONCLUSION

MD simulation method had been performed to investigate the diffusion behavior of hydrogen atoms into α-Fe. Diffusion and tension dynamics had been analyzed qualitatively and quantitively. Comparisons between our simulation results and experimental results from other researchers had been made. Main conclusions are as follows:

(1) Hydrogen atoms do not diffuse into the α-Fe with a perfect BCC structure. The existence of hydrogen trappings, such as vacancy facilitates the diffusion of adsorbed hydrogen into α-Fe.

(2) The ln$D$ displays a linear relation with 1/T, but with different slops at low temperatures ($T \leqq 300$ K) and high temperatures ($T > 300$ K).

(3) Loading enhances the diffusion behavior of hydrogen atoms.

(4) The high frequency of brittle fracture was found at the time scale from 210-220 K or at high vacancy concentration, especially C^V=3.48.

ACKNOWLEDGMENTS

This work is financial supported by the National Key Basic Research Program of China ("973 Program", Grant No. 2015CB057601). The authors gratefully acknowledge their team members Lin Zhang, Chengshuang Zhou, Zhengli Hua, Gai Huang and Wenmin Qu for fruitful discussion.

REFERENCES

1. Veziroglu, T.N. and Sahin, S., 21st Century's Energy: Hydrogen Energy System, *Energ. Convers Manage*, **49**, 7, 2008, 1820–1831.
2. Mao, Z.Q., Attention to Hydrogen Energy–the Most Development Potential Energy in the 21st Century, *China Sci. Technol Bus.*, **11**, 2004, 28–33.
3. Bryan, W.L. and Dodge, B.F., Diffusivity of Hydrogen in Pure Iron, *AIChE Journal*, **9**, 2, 1963, 223–228.
4. Heumann, T. and Domke, E., Hydrogen diffusion in Zone Melted α-Iron. *Berichte der Bunsengesellschaft für physikalische Chemie*, **76**, 8, 1972, 825–826.
5. Völkl, J. and Alefeld, G., Diffusion of Hydrogen in Metals, *Hydrogen in Metals I*, 1978, 321–348.
6. Hagi, H., Hayashi, Y. and Ohtani, N., Diffusion Coefficient of Hydrogen in Pure Iron Between 230 and 300 K, *Transactions of the Japan Institute of Metals*, **20**, 7, 1979, 349–357.
7. Nagano, M., Hayashi, Y., Ohtani, N., et al. Diffusion of Hydrogen and Deuterium in High Purity Iron between 222 and 322 K, *Transactions of the Japan Institute of Metals*, **22**, 6, 1981, 423–429.
8. Nagano, M., Hayashi, Y., Ohtani, N., et al. Hydrogen Diffusivity in High Purity Alpha Iron, *Scripta Metallurgica*, **16**, 8, 1982, 973–976.
9. Taketomi, S., Matsumoto, R. and Miyazaki, N., Atomistic Study of Hydrogen Distribution and Diffusion Around a {112}<111> Edge Dislocation in Alpha Iron, *Acta Materialia*, **56**, 15, 2008, 3761–3769.
10. Ramasubramaniam, A., Itakura, M., Ortiz, M., et al. Effect of Atomic Scale Plasticity on Hydrogen Diffusion in Iron: Quantum Mechanically Informed and on-the-fly Kinetic Monte Carlo Simulations, *Journal of Materials Research*, **23**, 10, 2008, 2757–2773.
11. Kiuchi, K. and McLellan, R.B., The Solubility and Diffusivity of Hydrogen in Well-Annealed and Deformed Iron, *Acta Metallurgica*, **31**, 7, 1983, 961–984.
12. Bruzzoni, P., Carranza, R.M., Lacoste, J.R.C., et al. Hydrogen Diffusion in α-Iron Studied Using An Electrochemical Permeation Transfer Function, *Electrochimica Acta*, **44**, 16, 1999, 2693–2704.
13. Nagumo, M., Function of Hydrogen in Embrittlement of High-Strength Steels, *ISIJ International*, **41**, 6, 2001, 590–598.
14. Nagumo, M., Nakamura, M. and Takai, K., Hydrogen Thermal Desorption Relevant to Delayed-Fracture Susceptibility of High-Strength Steels, *Metallurgical and Materials Transactions A*, **32**, 2, 2001, 339–347.
15. Tateyama, Y. and Ohno, T., Atomic-Scale Effects of Hydrogen in Iron Toward Hydrogen Embrittlement: Ab-Initio Study, *ISIJ International*, **43**, 4, 2003, 573–578.
16. Oriani, R.A. and Josephic, P.H., Equilibrium Aspects of Hydrogen-Induced Cracking of Steels, *Acta Metallurgica*, **22**, 9, 1974, 1065–1074.
17. Beachem, C.D., A New Model for Hydrogen-Assisted Cracking (Hydrogen "Embrittlement"), *Metallurgical Transactions*, **3**, 2, 1972, 441–455.
18. Birnbaum, H.K. and Sofronis, P., Hydrogen-Enhanced Localized Plasticity-A Mechanism for Hydrogen-Related Fracture, *Materials Science and Engineering: A*, **176**, 1–2, 1994, 191–202.
19. Fukai, Y. and Okuma, N., Evidence of Copious Vacancy Formation in Ni and Pd under A High Hydrogen Pressure, *Japanese Journal of Applied Physics*, **32**, 9A, 1993, L1256.
20. Fukai, Y. and Okuma, N., Formation of Superabundant Vacancies in Pd Hydride under High Hydrogen Pressures, *Physical Review Letters*, **73**, 12, 1994, 1640.

21. Fukai, Y., Formation of Superabundant Vacancies in M–H Alloys and Some of Its Consequences: A Review, *Journal of Alloys and Compounds*, **356**, 2003, 263–269.
22. Hayward, E. and Deo, C., Energetics of Small Hydrogen–Vacancy Clusters in BCC Iron, *Journal of Physics: Condensed Matter*, **23**, 42, 2011, 425402.
23. Lee, B.-J. and Jang, J.-W., A Modified Embedded-Atom Method Interatomic Potential for the Fe-H System, *Acta Mater.*, **55**, 2007, 6779–6788.
24. Plimpton, S., Fast Parallel Algorithms for Short-Range Molecular Dynamics, *J. Comput. Phys.*, **117**, 1, 1995, 1–19.
25. Shinoda, W., DeVane, R. and Klein, M.L., Coarse-Grained Molecular Modeling of Non-Ionic Surfactant Self-Assembly, *Soft Matter*, **4**, 12, 2008, 2454–2462.
26. LAMMPS (Large-scale Atomic/Molecular Massively Parallel Simulator); Software Available at http://lammps.sandia.gov.
27. Oriani, R.A., The Diffusion and Trapping of Hydrogen in Steel, *Acta Metallurgica*, **18**, 1, 1970, 147–157.